ELSEVIER

Thermochimica Acta 262 (1995) 145–155

thermochimica
acta

Studies on the kinetics of the carbothermic reduction of chromium oxide using the evolved gas analysis technique

M.P. Antony [a], R. Vidhya [a], C.K. Mathews [a,*], U.V. Varada Raju [b]

[a] *Fuel Chemistry Division, Chemical Group, IGCAR, Kalpakkam 603 102, India*
[b] *Materials Science Research Centre, Indian Institute of Technology, Madras 600036, India*

Received 8 December 1994; accepted 29 March 1995

Abstract

The kinetics of formation of Cr_3C_2 by the carbothermic reduction of Cr_2O_3 with graphite was studied in the temperature range 1461–1739 K. The experiments were carried out in a high vacuum chamber with the mechanically mixed reactants in pellet form, compacted at different pressures. The progress of the reaction was followed by monitoring the CO gas evolved by means of a quadrupole mass spectrometer. From the parabolic nature of the rate equation and the dependence of the activation energy of the reaction on the compaction pressure of the pellets, it was concluded that the diffusion of CO gas through the product layer was the rate-controlling step.

Keywords: Cr_3C_2; Graphite; Kinetics; Reduction

1. Introduction

Carbides of chromium are of interest because of the useful properties they impart to steels. Chromium reacts with carbon to form three carbides, Cr_3C_2, Cr_7C_3 and $Cr_{23}C_6$[1]. The precipitation of these compounds plays an important role in controlling the chemical and physical properties of some high-chromium steels and super alloys. The most widely used method for producing chromium carbides is by the reaction of the oxide with carbon [2] under high vacuum conditions.

The kinetics of solid state reactions are usually studied either by measuring the weight loss of a sample or by monitoring the growth of one of the products as a function

---

* Corresponding author.

SSDI 0040-6031(95)02407-7

of time at different temperatures. In this paper, we report a study of the kinetics of the carbothermic reduction of Cr_2O_3 by continuously measuring the amount of CO evolved using a quadrupole mass spectrometer (QMS). The overall reaction is represented by the equation

$$3Cr_2O_3(s) + 13C(s) \longrightarrow 2Cr_3C_2(s) + 9CO(g) \qquad (1)$$

The rate of reaction, derived from the rate of release of CO, was analysed to understand the reaction mechanism.

2. Experimental

2.1. Experimental assembly

The experimental system used for carrying out the reaction consisted of a stainless steel high vacuum chamber with provisions for sample heating and pressure measurements. Fig. 1 shows the details of the equipment. This sample in the form of a pellet was inserted into a molybdenum crucible and heated by an RF induction coil. The sample temperature was monitored using an infrared pyrometer (Landmark X, USA). The gases evolved during the reaction were measured quantitatively using a quadrupole mass spectrometer (Spectramass, DAQ 200/DXS). The total pressure in the chamber was monitored by an ion-gauge and a spinning rotary gauge (SRG). The base pressure achievable in the vacuum system was about 1×10^{-7} Torr.

The calibration of the QMS was carried out by heating known amounts of calcium carbonate and calcium oxalate [3] and measuring the partial pressures of CO and CO_2 gases evolved during the thermal decomposition of $CaCO_3$ and CaC_2O_4. The calibration constants for the partial pressures of CO and CO_2, p_{CO} and p_{CO_2}, were found to be 163.9 and 191.502 μmol Pa^{-1} s^{-1} respectively.

2.2. Sample preparation

Stoichiometric amounts of highly pure (99.99%) Cr_2O_3 and spectroscopic grade graphite powder (M/S. Ultra Carbon Corpn., USA) were blended together in an agate mortar for about 45 min. The blend was then compacted using a press to obtain pellets 6 mm in diameter, 1 mm thick, and weighing about 90–100 mg. The weight of each sample was kept uniform in order to compare the results. Sample pellets were prepared by compacting the mixture at pressures gauge of 5, 10, 15 and 20 MPa. All the pellets were degassed at around 423 K to remove moisture as well as the residual gases present in the sample.

3. Results

3.1. Reaction rate measurement

Each sample pellet was inserted into a molybdenum crucible and then heated rapidly to the desired temperature (1461–1739 K) in the vacuum system. Before heating the

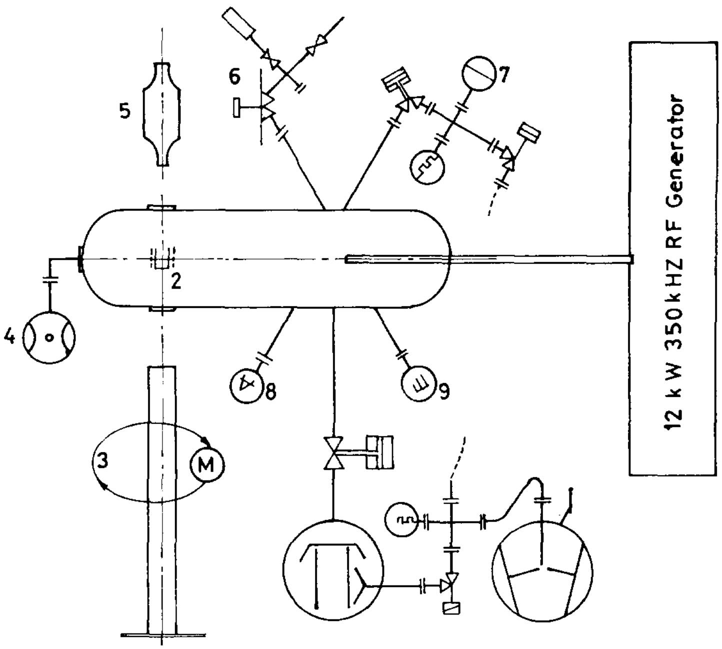

1. UHV Chamber
2. Induction coil and coaxial feed
3. Sample transfer device
4. Spinning rotor gauge
5. Fibroptic radiation pyrometer
6. Thermomechanical leak valve
7. Capacitance monometer
8. B A Ion guage
9. Quadrupole mass analyzer

Fig. 1. Details of the experimental assembly.

sample, the vacuum chamber was purged with argon gas and then baked in order to attain a stable, low background for CO and CO_2.

The partial pressure of carbon monoxide was measured at $m/z = 28$. In order to avoid the problem of isobaric interference from N_2 at this mass number, the following precautions were taken. The chamber was evacuated for several hours to obtain a stable background pressure at $m/z = 28$. All the pressure measurements were made at pressures at least two orders above the background. The background pressure was then subtracted from the signal in all the calculations. This ensured that there was no contribution from residual N_2 in the chamber to the measured CO pressures. The ion intensity at mass 14 was periodically monitored at a higher electron impact energy to rule out the contribution of N_2 at mass 28. It was also found that the amounts of CO_2 released from the sample were negligible.

After carrying out the reaction for a given time at the specified temperature, the pellets were weighed and the weight loss during reaction was recorded.

The reaction ratio, which is the fraction of the oxide converted to the carbide in a given time, was estimated by two methods. In the first method, α was calculated as the ratio of the amount of CO gas evolved in a given time during the reaction to the total amount of CO that would have evolved on completion of the reaction. The peak area under the partial pressure–time curve corresponds to the amount of gas evolved. In the second method, α was calculated as the ratio of the weight loss of the sample in a given time to the total weight loss expected when the reaction was completed, i.e.

$$\alpha = (W_0 - W_t)/(W_0 - W_f)$$

where W_0, W_t and W_f are the initial weight, weight at time t, and final weight of the sample respectively.

The reaction ratio calculated from peak area measurements for a pellet compacted at 5 MPa pressure and heated at 1523 K is shown in Table 1. The reaction ratio calculated by the weight loss method was found to be in good agreement with that estimated by the evolved gas analysis method. Typical plots of reaction ratios against time and temperature at different pelletisation pressures are shown in Figs. 2 and 3.

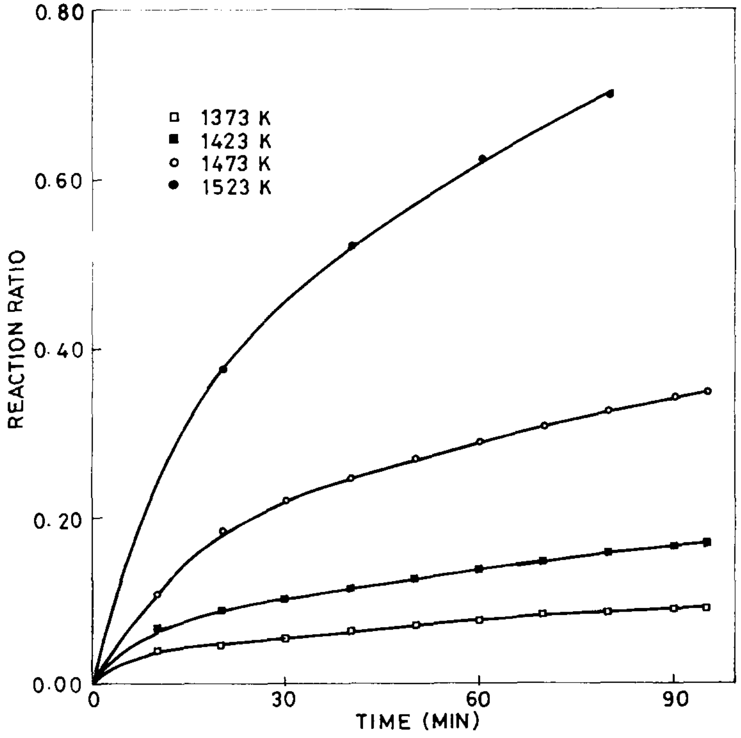

Fig. 2. Plot of reaction ratio against time at different temperatures.

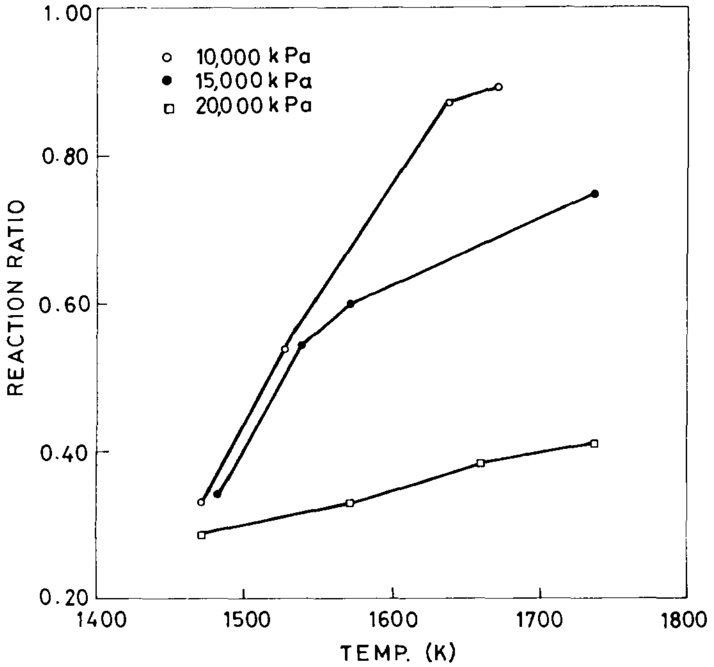

Fig. 3. Plot of reaction ratio against temperature for pellets compacted at different pressures.

Table 1
Calculation of reaction ratio at 1523 K for a pellet compacted at 5 MPa pressure; sample weight, 94.62 mg

Time/min	Peak area/(Torr s)	Moles of CO	Reaction ratio α
20	1.1097E-2	298.112	0.3776
40	4.2420E-3	113.955	0.5219
60	2.8830E-3	77.447	0.6205
80	2.2185E-3	59.597	0.6955
100	1.5510E-3	41.665	0.7483
120	1.2690E-3	34.089	0.7915
140	1.0553E-3	28.348	0.8274

3.2. Intermediate phase identification

The pellets, after reaction, were crushed to powder and the powder was analysed by X-ray diffractometry using Mo Kα radiation to identify the final products as well as intermediate phases, if any. The X-ray diffraction patterns of the powder samples, as shown in Fig. 4, indicate that the reaction progressed as expected from the results of

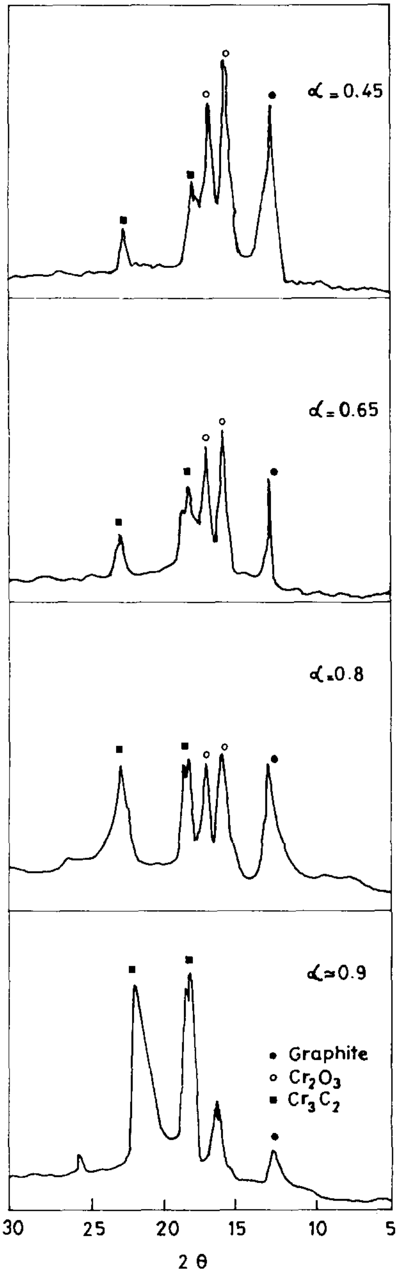

Fig. 4. X-ray diffraction patterns for the products of reaction ratios of 0.45, 0.65, 0.8 and 0.9.

reaction ratio measurements. The X-ray pattern for a sample with $\alpha = 0.45$ exhibits the presence of Cr_2O_3 and graphite as the main constituents and Cr_3C_2 phase as a trace constituent. As the reaction ratio increased the relative amounts of Cr_2O_3 and graphite phases decreased and at $\alpha = 0.9$ these two phases almost disappeared. Only the Cr_3C_2 phase remained at detectable levels.

4. Discussion

4.1. Reaction mechanism

Various models have been proposed to describe the kinetics of solid state reactions. Sestak [4] has proposed some models to describe the kinetics as well as the mechanism of solid state reactions in general. Lindemer et al. [5] studied the kinetics of the carbothermic reduction of uranium oxide and discussed two models: (i) a geometrically uniform model which is considered when the heating rate is low, and (ii) a geometrically non-uniform model which should be considered when the heating rate is very high. Because we adopted a rapid heating process, the non-uniform model appears to be more appropriate in the present study. Stinton et al. [6] postulated that, in the case of such reactions, surface nucleation takes place instantaneously and the particle is covered by a thin layer of the product; the rate-determining process becomes the propagation of the reaction interface to the center of the particle, controlled by either reaction at the interface or diffusion of CO through the product layer.

4.2. Interface-controlled reactions

When diffusion through the product layer is so rapid that the reactants cannot combine fast enough at the reaction interface to establish equilibrium, the process becomes interface-controlled. In these cases the reaction rate is proportional to the surface area of the fraction of the unreacted material, and the rate equation can be given as

$$d\alpha/dt = kS_t/V_0$$

where α is the reaction ratio, S_t is the surface area of the unreacted core particle, and V_0 is the original volume of the particle.

After various mathematical operations, the above equation is transformed to the form given by Spencer and Topley [7]

$$[1-(1-\alpha)^{1/3}] = kt/r_0$$

where k is the rate constant and r_0 is the radius of the particle.

4.3. Diffusion-controlled reactions

When the penetration of one of the reactants through the product layer is the rate-controlling process, then the time dependence of a gradual build-up of the planar product layer is inversely proportional to its thickness

$$dy/dt = k/y$$

where y is the thickness of the product layer. Jander [8] applied the parabolic rate law and derived the rate equation

$$[1-(1-\alpha)^{1/3}]^2 = 2kDt/[r_0]^2$$

where k is the proportionality constant and r_0 is the radius of the particle. This equation becomes equivalent to the equation

$$[1-(1-\alpha)^{1/3}]^2 = kt$$

when (a) there is an instantaneous surface nucleation, (b) there is bulk diffusion in all directions, (c) there is immiscibility of the product phase with any one of the reactant phases, and (d) the reactant particles are spheres of uniform radii.

The present results can be best fitted to Jander's equation for diffusion-limited kinetics [8]. The plots of $[1-(1-\alpha)^{1/3}]$ and $[1-(1-\alpha)^{1/3}]^2$ as a function of time are shown in Fig. 5. of the two, Jander's equation for diffusion-limited kinetics, best fits the

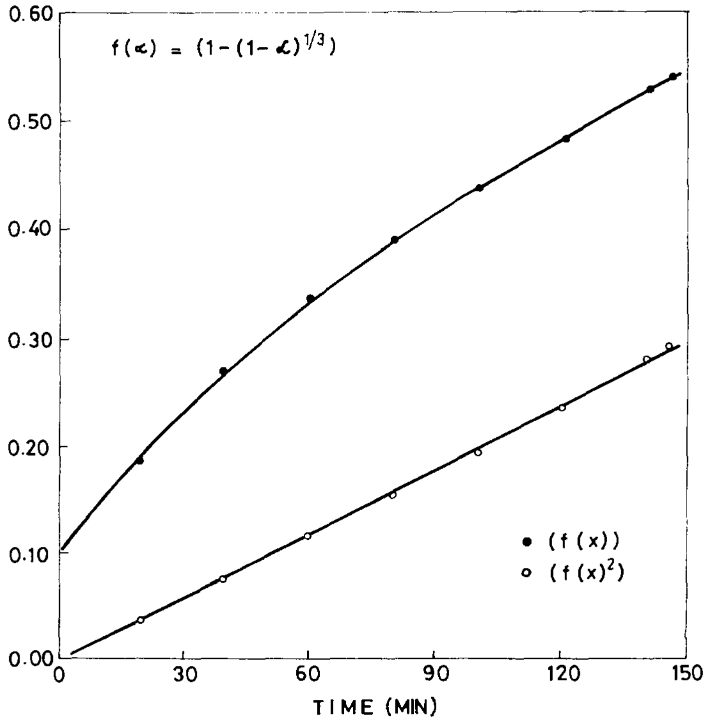

Fig. 5. Plot of $[(1-(1-\alpha)^{1/3}]$ and $[(1-(1-\alpha)^{1/3}]^2$ against time.

present data. This suggests that the rate-controlling process of the carbothermic reduction of Cr_2O_3 could be the diffusion of carbon and oxygen in the solid phase or that of carbon monoxide in the gas phase. It was observed that the rate of reaction decreased as the compaction pressure of the pellet increased. If the diffusion of carbon or oxygen in the solid state were the rate-determining step, the reaction rate would have increased with an increase in the pelletisation pressure. Hence, it is concluded that the diffusion of CO gas through the product layer or in the gas phase is much slower than the solid state diffusion of oxygen or carbon, and thus controls the rate of the reaction.

These results are consistent with Lindemer et al.'s [5] non-uniform model. In this model small uniform microspheres of Cr_2O_3 are initially surrounded by carbon. The reaction takes place in the interface region between Cr_2O_3 and C. This reaction zone is initially at the particle surface, but as the reaction proceeds, the interface shifts slowly towards the centre of the particle. Cr_2O_3 near the interface reacts readily with carbon to form Cr_3C_2. The CO gas released at the interface will diffuse through the product layer to the particle surface. The Cr_3C_2 layer grows laterally until the entire particle is almost completely converted to Cr_3C_2.

The CO generated in the interface region must diffuse through the product layer in the particle and then through the intergranular pathways in the pellet before it emerges out into the vacuum chamber. The fact that the pellets compacted at lower pressures reacted much faster than the pellets compacted at higher pressures suggests that the bulk diffusion of CO in the pellet also plays a role in the rate of the reaction. Hence either of the above diffusion processes or both together could be the rate-limiting step in the reaction.

Thus, it is reasonable to assume that, at the high heating rates employed in the study, CO gas is produced in large amounts at the Cr_3C_2–Cr_2O_3 interface. The extent of conversion of Cr_2O_3 to Cr_3C_2 depends on the removal of this CO to the surface of the particle. The pressure of CO inside the pellet is likely to be quite high and a pressure gradient exists between the centre of the pellet and the surface. The CO diffuses to the surface through the interconnected pores in the pellet.

The activation energy of the reaction can help to identify the diffusion process. Arrhenius plots of reaction rate constant k against $1/T$ for pellets compacted at different pressures are shown in Fig. 6. The rate equations that linearly fit the data points and the average activation energy are given in Table 2. It is seen that the activation energy increases with pelletisation pressure. This indicates that CO diffusion through the product layer is the rate-determining step. In the sintered pellet, CO pressure builds up in the pores, thus slowing down CO diffusion.

Table 2
Rate equations and energy of activation

Pellet pressures/kPa	Rate equations	Activation energy/(kJ mol^{-1})
10,000	$\ln k = -22530.5/T + 6.8$	185
15,000	$\ln k = -30507.9/T + 12.3$	255
20,000	$\ln k = -35910.7/T + 14.7$	300

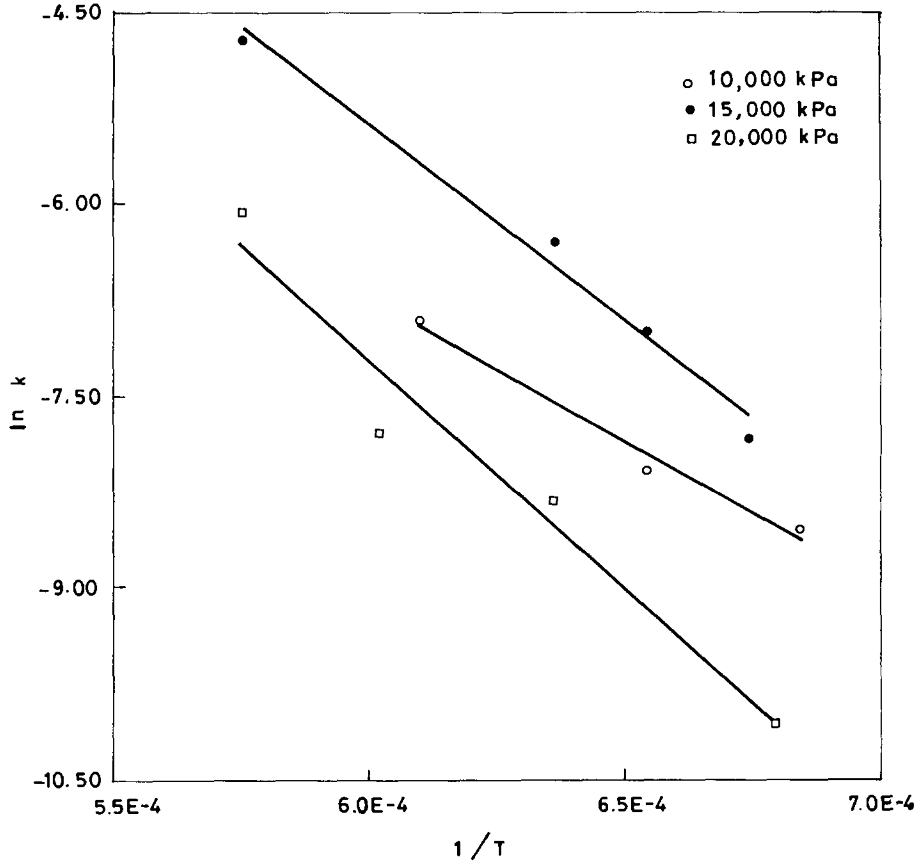

Fig. 6. Arrhenius plot of reaction rate constant k against $1/T$, for pellets compacted at different pressure: 1, 10000 kPa; 2, 15000 kPa; 3, 20000 kPa.

5. Conclusions

The kinetics of formation of Cr_3C_2 from a mixture of Cr_2O_3 and graphite has been studied by the evolved gas analysis method for the first time. In this method, the sample was heated in a high vacuum chamber and one of the reaction products, CO gas, was measured quantitatively using a quadrupole mass spectrometer. The reaction ratio α was calculated from CO measurements. The α values were calculated from weight loss measurements separately. The fact that both values agree very well suggests that the evolved gas analysis method can be effectively used for studying the kinetics of chemical reactions wherein one of the products is a gas. The advantage of using quadrupole mass spectrometry is that even the occluded gases present in the sample can be detected and measured.

The increase in activation energy of the reaction as the compaction pressure of the pellets increased suggests that the rate-determining step of the carbothermic reduction of Cr_2O_3 with graphite to make Cr_3C_2 is controlled by the diffusion of CO gas from the reaction interface to the surface of the pellet.

Acknowledgements

The authors thank Dr. S. Rajagopalan for help in the characterisation of the samples by X-ray diffractometry. The encouragement and support of Dr. P.R. Vasudeva Rao, Head Fuel Chemistry Division, while carrying out this work is gratefully acknowledged.

References

[1] E.K. Storms, The Refractory Carbides, Academic Press, New York, 1967, p. 136.
[2] T. Ya. Kosolapova, Carbides: Properties, Production and Applications, Plenum Press, New York, 1971.
[3] J. Wang and B. McEnaney, Thermochim. Acta, 190 (1991) 143.
[4] J. Sestak, in Thermal Analysis, Vol. III, Proc. 3rd ICTA, Davos, 1971.
[5] T.B. Lindemer, M.D. Allen and J.M. Leitnaker, J. Am. Ceram. Soc., 52 (1969) 233.
[6] D.P. Stinton, S.M. Tiegs, W.J. Lackey and T.B. Lindemer, J. Am. Ceram. Soc., 62 (11–12) (1979) 596.
[7] W.D. Spencer and B. Topley, J. Chem. Soc., (1929) 2633.
[8] W. Jander, Z. Anorg. Allg. Chem., 163 (1927) 1.